

SCHOOL OF COMPUTER SCIENCE, NORTHWESTERN POLYTECHNICAL UNIVERSITY

---

# *r*-HUMO: A Risk-Aware Human-Machine Cooperation Framework for Entity Resolution with Quality Guarantees

---

Boyi Hou, Qun Chen, Zhaoqiang Chen, Youcef Nafa, Zhanhuai Li

May 16, 2018

Even though many approaches have been proposed for entity resolution (ER), it remains very challenging to find one with quality guarantees. To this end, we propose a *r*-isk-aware HUman-Machine cOoperation framework for ER, denoted by *r*-HUMO. Built on the existing HUMO framework, *r*-HUMO similarly enforces both precision and recall levels by partitioning an ER workload between the human and the machine. However, *r*-HUMO is the first solution to optimize the process of human workload selection from a risk perspective. It iteratively selects human workload based on real-time risk analysis on human-labeled results as well as pre-specified machine metrics. In this paper, we first introduce the *r*-HUMO framework and then present the risk analysis technique to prioritize the instances for manual labeling. Finally, we empirically evaluate *r*-HUMO’s performance on real data. Our extensive experiments show that *r*-HUMO is effective in enforcing quality guarantees, and compared with the state-of-the-art alternatives, it can achieve better quality control with reduced human cost.

## 1 INTRODUCTION

Entity resolution (ER) usually refers to identifying the relational records that correspond to the same real-world entity. A challenging task due to incomplete and dirty data, ER has been extensively studied in the literature [1, 2]. Unfortunately, most of the existing approaches [3, 4, 5, 6,

7, 8, 9, 10, 11] cannot enforce quality guarantees. Note that the approach based on active learning [12, 13] can maximize recall while ensuring a pre-specified precision level. More recently, a HUMAN-Machine cOoperation framework [14, 15], denoted by HUMO, has been proposed to enforce more comprehensive quality guarantees at both precision and recall fronts. HUMO enables a flexible mechanism for quality control by partitioning an ER workload between the human and the machine. It automatically labels easy instances by the machine while assigning more challenging ones to the human. For instance, given a metric of record pair similarity, the pairs with high or low similarities can be automatically labeled by the machine with high accuracy. However, the pairs with medium similarities may require human verification because labeling them either way by machine would introduce considerable errors. The optimization objective of HUMO is to minimize the required human cost given user-specified precision and recall levels.

HUMO measures the hardness of an ER instance pair by a pre-specified machine metric and performs human workload selection in batch mode. It first groups the pairs into subsets by their metric values and then assigns the subsets between the human and the machine. As a result, all the pairs with similar metric values in a subset would be either automatically labeled by the machine or manually labeled by the human. However, it can be observed that due to the limitation of machine metrics, even though two pairs have similar metric values, their risks of being mislabeled by the machine may be vastly different.

In this paper, we investigate the problem of workload partition between the human and the machine from a risk perspective. Since human workload selection can be performed in an interactive manner, human input, which consists of the human-labeled pairs in our example, can be naturally used for risk analysis to prioritize pairs for human verification. Our idea is to iteratively pick up more risky pairs from a given subset of pairs for human verification such that the remaining pairs in the subset can achieve overall higher machine-labeling accuracy. With human effort spent on more risky pairs, the required human cost for quality guarantees can be effectively reduced. As HUMO, the proposed risk-aware framework, *r*-HUMO, is to some extent motivated by the success of the existing crowdsourcing solutions for ER [16, 17, 18, 19]. The work on crowdsourcing ER focused on how to make the human work effectively and efficiently on a given workload. HUMO and *r*-HUMO instead investigate how to partition a workload between the human and the machine such that a user-specified quality requirement can be met.

The major contributions of this paper can be summarized as follows:

1. We propose a risk-aware human-machine cooperation framework for ER, *r*-HUMO, which can ensure both precision and recall guarantees. It is the first solution to optimize the process of human workload selection from a risk perspective.
2. We propose the technique of risk analysis for iterative human workload selection. We present the risk models based on modern portfolio investment theory to prioritize ER pairs for human verification.
3. We conduct an empirical study on the performance of *r*-HUMO by extensive experiments on real data. Our experimental results show that *r*-HUMO is effective in enforcing quality guarantees, and compared with the state-of-the-art alternatives, it can achieve better quality control with reduced human cost.

The rest of this paper is organized as follows: Section 2 reviews more related work. Section 3 introduces the problem and briefly describes the existing HUMO framework. Section 4 presents the  $r$ -HUMO framework. Section 5 presents the risk analysis technique. Section 6 presents our empirical evaluation results. Finally, Section 7 concludes this paper with some thoughts on future work.

## 2 RELATED WORK

As a classical problem in the area of data quality, entity resolution has been extensively studied in the literature [1, 2]. It can be performed based on rules [4, 5, 6], probabilistic theory [3, 20] or machine learning [7, 8, 12, 13]. However, these traditional techniques lack effective mechanisms for quality control, therefore can not enforce quality guarantees.

The approaches based on active learning [12, 13] have been proposed to enforce the precision requirement for ER. The authors of [12] proposed a technique that can optimize recall while ensuring a pre-specified precision level. The authors of [13] proposed an improved algorithm to approximately maximize recall under the precision constraint. Its major advantage over that of [12] is better label complexity. However, these techniques share the same classification paradigm with the traditional machine learning-based ones, hence, they can not enforce comprehensive quality guarantees specified at both precision and recall fronts.

The progressive paradigm for ER [21, 22] has also been proposed for the application scenarios in which ER should be processed efficiently but does not necessarily require to generate high-quality results. Taking a pay-as-you-go approach, it studied how to maximize result quality given a pre-specified resolution budget. In [21], the authors proposed several concrete ways of constructing resolution “hints” that can be then used by a variety of existing ER algorithms as a guidance for which entities to resolve first. In [22], the authors studied the more complicated problem of relational ER, in which a resolution of some entities might influence the resolution of other entities. A similar iterative algorithm, SiGMA, was proposed in [23]. It can leverage both the structure information and string similarity measures to resolve entity alignment across different knowledge bases. There also exists some interactive systems [26, 34] that take advantage of knowledge bases or specific user input to achieve improved efficiency and quality for data cleaning. Having been built on machine computation, these techniques could not be applied to enforce quality guarantees either.

It has been well recognized that pure machine algorithms may not be able to produce satisfactory results in many practical scenarios [17]. Many researchers [9, 16, 18, 19, 24, 25, 26, 27, 28, 29, 30, 31] have studied how to crowdsource an ER workload. In [18], the authors studied how to generate Human Intelligence Tasks (HIT), and how to incrementally select the instance pairs for human verification such that the required human cost can be minimized. In [28], the authors focused on how to select the most beneficial questions for humans in terms of expected accuracy. More recently, the authors of [16] proposed a cost-effective framework that employs the partial order relationship on instance pairs to reduce the number of asked pairs. Similarly, the authors in [31] provided solutions to take advantage of both pairwise and multi-item interfaces in a crowdsourcing setting. The authors of [32] studied how to balance cost and quality in crowdsourcing. Considering the diverse accuracies of workers across tasks, the authors of [33]

proposed an adaptive crowdsourcing framework that assigns tasks based on worker accuracy estimation. In [27], the authors proposed an online crowdsourcing platform based on oracle. While, these works addressed the challenges specific to crowdsourcing; this paper instead investigate a different problem: how to partition a workload between the human and the machine such that the user-specified quality guarantees can be met. Note that the workload assigned to the human by *r*-HUMO can be naturally processed in a crowdsourcing manner. Our work can thus be considered orthogonal to the existing works on crowdsourcing. It is interesting to investigate how to seamlessly integrate a crowdsourcing platform into *r*-HUMO in future work.

The *r*-HUMO framework is built on the recently proposed HUMO framework [14, 15], which can enforce quality guarantees at both precision and recall fronts. It is however the first solution to optimize the process of human workload selection from a risk perspective. Instead of selecting human workload in batch mode purely based on a pre-specified machine metric as HUMO does, *r*-HUMO performs real-time risk analysis on manually labeled results for the purpose of reducing the required human cost.

### 3 PRELIMINARIES

#### 3.1 PROBLEM DEFINITION

Entity resolution reasons about whether two records are equivalent. Two records are deemed to be equivalent if and only if they correspond to the same real-world entity. We call a pair a *matching* pair if its two records are equivalent; otherwise, it is called an *unmatching* pair. An ER solution corresponds to a label assignment for a set of record instance pairs. The label of a pair indicates that the two records in the pair are *matching* or *unmatching*. As usual, we measure the quality of an ER solution by the metrics of precision and recall. Precision is the fraction of matching pairs among the pairs labeled as *matching*, while recall is the fraction of correctly labeled matching pairs among all the matching pairs. Formally, we denote the ground-truth labeling solution of  $D$  by  $\hat{L}$ ,  $\hat{L} = \{\hat{l}_1, \hat{l}_2, \dots, \hat{l}_n\}$ , in which  $\hat{l}_i = 1$  if the corresponding records in the pair of  $d_i$  are equivalent and  $\hat{l}_i = 0$  otherwise. Given a labeling solution  $L$ , we use  $D_{tp}$  to denote its set of true positive pairs,  $D_{tp} = \{d_i | \hat{l}_i = 1 \wedge l_i = 1\}$ ,  $D_{fp}$  its set of false positive pairs,  $D_{fp} = \{d_i | \hat{l}_i = 0 \wedge l_i = 1\}$ , and  $D_{fn}$  its set of false negative pairs,  $D_{fn} = \{d_i | \hat{l}_i = 1 \wedge l_i = 0\}$ . Based on the definitions of  $D_{tp}$ ,  $D_{fp}$  and  $D_{fn}$ , the achieved precision level of  $L$  can be represented by

$$precision(D, L) = \frac{|D_{tp}|}{|D_{tp}| + |D_{fp}|}. \quad (1)$$

Similarly, the achieved recall level of  $L$  can be represented by

$$recall(D, L) = \frac{|D_{tp}|}{|D_{tp}| + |D_{fn}|}. \quad (2)$$

We define the problem of entity resolution with quality guarantees [14] as follows:

**Definition 1** *[Entity Resolution with Quality Guarantees]* Given a set of instance pairs,  $D = \{d_1, d_2, \dots, d_n\}$ , the problem of entity resolution with quality guarantees is to give a labeling

solution  $L$  for  $D$  such that with a confidence level of  $\theta$ ,  $\text{precision}(D, L) \geq \alpha$  and  $\text{recall}(D, L) \geq \beta$ , in which  $\alpha$  and  $\beta$  denote the user-specified precision and recall levels respectively.

### 3.2 THE HUMO FRAMEWORK

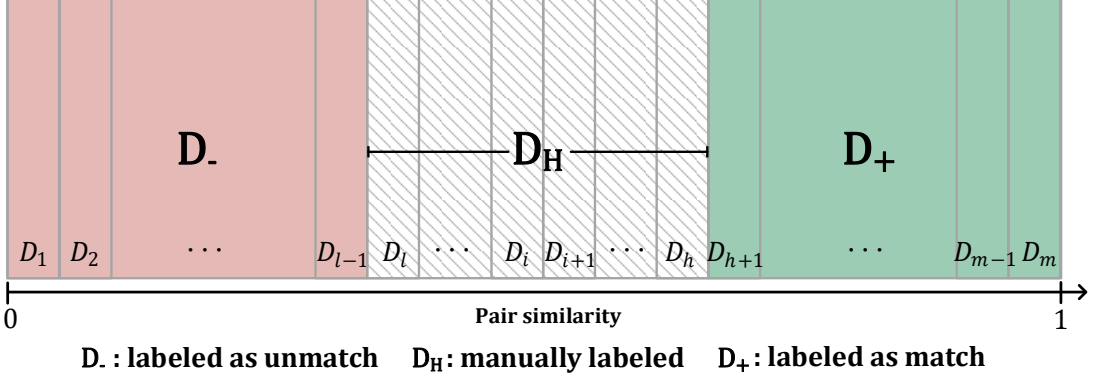


Figure 1: HUMO Framework.

The HUMO framework is shown in Fig. 1. Given a set of instance pairs,  $D$ , HUMO first groups the pairs into unit subsets (denoted by  $D_i$  in the figure) by a machine metric (i.e. pair similarity or match probability), and then partitions the unit subsets into three disjoint sets,  $D_-$ ,  $D_H$  and  $D_+$ . HUMO assumes that the given machine metric satisfies the monotonicity of precision, which statistically states that the higher (or lower) metric values a set of pairs have, the more probably they are matching pairs. *Note that the monotonicity assumption of precision underlies the effectiveness of existing machine classification metrics for ER. HUMO enforces the precision and recall levels by automatically labeling  $D_-$  and  $D_+$  as unmatching and matching respectively, and assigning  $D_H$  to the human for manual verification. It is worthy to point out that HUMO is effective provided that the given machine metric satisfies the monotonicity assumption of precision. For the sake of presentation simplicity, we use pair similarity as the example of machine metric in this paper.*

The quality of a HUMO solution  $S$  can be estimated by reasoning about the lower and upper bounds of the number of matching pairs in  $D_-$ ,  $D_H$  and  $D_+$ . In Figure. 1, the lower bound of the achieved precision level can be represented by

$$\text{precision}_l(S) = \frac{N_l^+(D_+) + N_l^+(D_H)}{N(D_+) + N(D_H)}, \quad (3)$$

in which  $N(\cdot)$  denotes the total number of pairs in a set and  $N_l^+(\cdot)$  denotes the lower bound of the total number of matching pairs in a set. Similarly, the lower bound of the achieved recall level can be represented by

$$\text{recall}_l(S) = \frac{N_l^+(D_+) + N_l^+(D_H)}{N_l^+(D_+) + N_l^+(D_H) + N_u^+(D_-)}, \quad (4)$$

in which  $N_u^+(\cdot)$  denotes the upper bound of the total number of matching pairs in a set. *In this paper, for the sake of presentation simplicity, we assume that the pairs in  $D_H$  can be manually labeled with 100% accuracy. However, it is worthy to point out that the effectiveness of HUMO does not depend on the 100%-accuracy assumption. It can actually work properly provided that quality guarantees can be enforced on  $D_H$ . In the case that human errors are introduced in  $D_H$ , the lower bounds of the achieved precision and recall can be similarly estimated based on Eq. 3 and Eq. 4.* Nonetheless, under the assumption that the human performs better than the machine in resolution quality, the best quality guarantees HUMO can achieve are no better than the performance of the human on  $D_H$ .

As human work is usually more expensive than machine computation, HUMO aims to minimize the workload in  $D_H$  while guaranteeing labeling quality. By quantifying human cost by the number of instance pairs in  $D_H$ , we define the optimization problem of HUMO as follows [14]:

**Definition 2 [Minimizing Human Cost in HUMO].** *Given a set of instance pairs  $D$ , a confidence level  $\theta$ , a precision level  $\alpha$  and a recall level  $\beta$ , the optimization problem of HUMO is represented by*

$$\begin{aligned} & \underset{S_i}{\operatorname{argmin}}(|D_H(S_i)|) \\ & \text{subject to } P(\text{precision}(D, S_i) \geq \alpha) \geq \theta, \\ & \quad P(\text{recall}(D, S_i) \geq \beta) \geq \theta, \end{aligned} \quad (5)$$

in which  $S_i$  denotes a labeling solution,  $D_H(S_i)$  denotes the set of instance pairs assigned to the human by  $S_i$ ,  $\text{precision}(D, S_i)$  denotes the achieved precision level of  $S_i$ , and  $\text{recall}(D, S_i)$  denotes the achieved recall level of  $S_i$ .

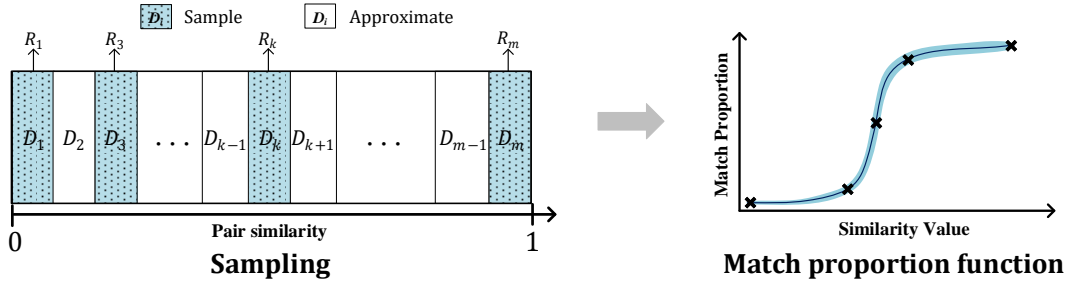


Figure 2: Process of GPR.

The optimization problem as defined in Eq. 5 is challenging due to the fact that the match proportions of the instance pairs in  $D_+$  and  $D_-$  are unknown, thus require to be estimated. There exists two types of approaches to minimize the size of  $D_H$ : one purely based on the monotonicity assumption of precision and the other one based on sampling [14, 15]. They estimate the match proportions of  $D_+$  and  $D_-$  based on different assumptions. Between them, the sampling-based approach has been empirically shown to have superior performance. It first estimates the match proportions of the unit subsets of  $D_i$  by sampling, then identifies the minimal workload

of  $D_H$  by reasoning about the numbers of matching pairs in  $D_-$  and  $D_+$ . The match proportion of a unit subset,  $D_i$ , can be directly estimated by sampling  $D_i$  or approximated by Gaussian Process Regression (GPR) [35]. The process of GPR is shown in Fig. 2. By assuming that the match proportions of all the subsets have a joint Gaussian distribution, GPR can approximate the match proportions of all unit subsets by sampling only a fraction of them. Representing the distributions of the match proportions of unit subsets by Gaussian functions, HUMO can estimate the lower and upper bounds of the numbers of matching pairs in  $D_-$  and  $D_+$  by aggregating their corresponding Gaussian distributions. It can therefore iteratively optimize the lower and upper bounds of  $D_H$ . More technical details of HUMO can be found at [14].

## 4 THE $r$ -HUMO FRAMEWORK

The  $r$ -HUMO framework consists of two processes, human workload selection and risk analysis. The process of human workload selection picks the pairs for manual verification from a set of candidate pairs; the process of risk analysis estimates pair risk based on the human-labeled results. The procedure is invoked iteratively until the user-specified quality requirements are met. After each iteration, the set of candidate pairs is updated and pair risk is also re-estimated based on the updated human-labeled results. The  $r$ -HUMO framework and its workflow are shown in Fig. 3.

In the rest of this section, we first describe the process of human workload selection provided with a risk model, and then present the technical details of quality assurance. The technique of risk analysis will be presented in the following section.

### 4.1 HUMAN WORKLOAD SELECTION

Suppose that  $D$  has been divided into  $m$  unit subsets with increasing metric values of pair similarity,  $D = \{D_1, D_2, \dots, D_m\}$ . Initially, we set  $D_H = \emptyset$ ,  $D_- = \{D_1, \dots, D_i\}$ , and  $D_+ = \{D_{i+1}, D_{i+2}, \dots, D_m\}$ . Since the pairs in  $D_-$  would be automatically labeled as *unmatch*, the match proportions of the subsets in  $D_-$  are expected to be less than 0.5; similarly, the match proportions of the subsets in  $D_+$  are expected to be larger or equal to 0.5.

Similar to HUMO,  $r$ -HUMO alternately picks the pairs in  $D_-$  and  $D_+$  for manual verification to enforce precision and recall guarantees. In the rest of this subsection, we first describe the processes of pair selection on  $D_-$  and  $D_+$ , and then present the algorithm to enforce quality guarantees based on them.

**Pair Selection in  $D_-$ .** According to the monotonicity assumption of precision, the pairs in  $D_i$  (the rightmost subset in  $D_-$ ) have higher probabilities of being *matching* than any other subset in  $D_-$ . Accordingly, they are at more risk to be mislabeled by the machine. Therefore,  $r$ -HUMO sets the initial candidate pair set, denoted by  $D_l$ , to be  $D_i$ , or  $D_l = D_i$ . It then iteratively selects the pairs in  $D_l$  in a risk-wise decreasing order for human verification. We represent the Marginal Match Proportion (MMP) of selection by

$$MMP(D_l) = \frac{dM}{dN}, \quad (6)$$

in which the variables  $N$  and  $M$  represent the number of inspected pairs and the number of matching pairs among them respectively. It can be observed that if risk estimation is effective,

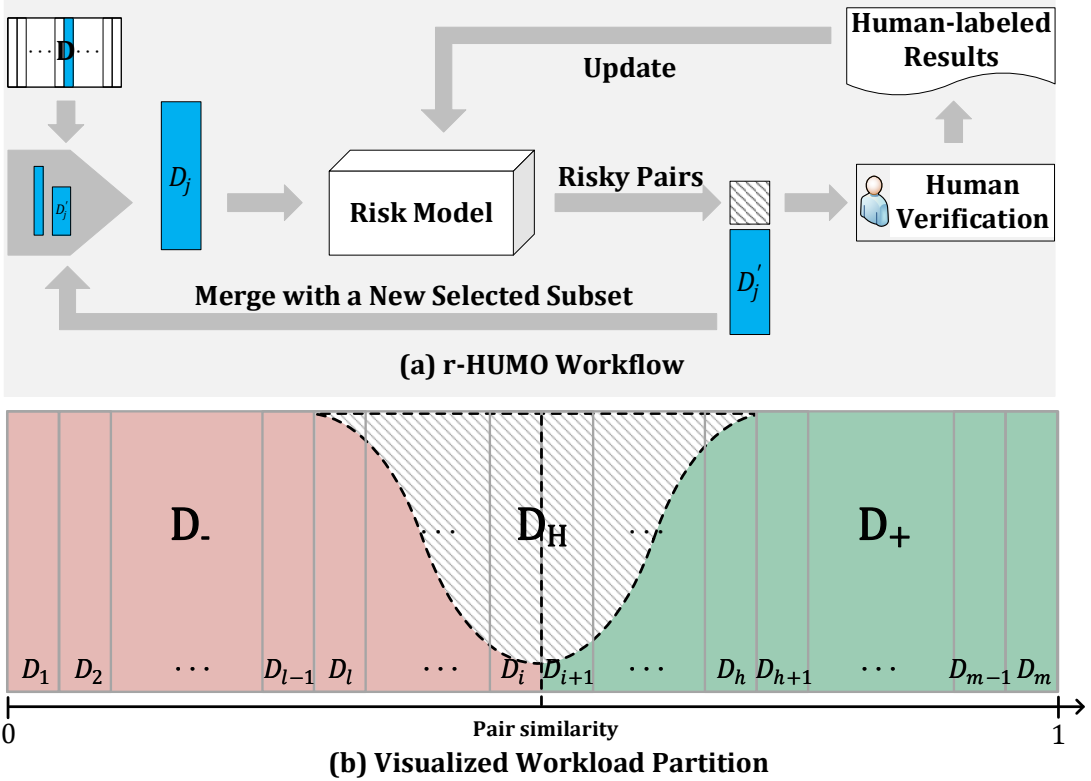


Figure 3: *r*-HUMO Framework.

$MMP(D_l)$  would decrease as the selection proceeds. For simplicity of presentation, we denote the expected match proportion of a subset  $D_l$  by  $E(D_l)$ , and the set of remaining pairs in  $D_l$  by  $D'_l$ . Iterative pair selection on  $D_l$  would stop once either one of the two following conditions is satisfied:

1. The expected match proportion of the remaining pairs in  $D'_l$  falls equal to or below the expected match proportion of the rightmost uninspected unit subset adjacent to  $D_l$  in  $D_-$ . Denoting the rightmost subset by  $D_j$ , we have  $E(D'_l) \leq E(D_j)$ ;
2. The marginal match proportion of selection,  $MMP(D_l)$ , falls equal to or below the expected match proportion of the remaining pairs in  $D_l$ , or  $MMP(D_l) \leq E(D'_l)$ .

It can be observed that if the first condition is triggered, the pairs mislabeled by the machine can be more easily found in the unit subset  $D_j$  instead of  $D'_l$ . If the second condition is triggered, risk analysis on  $D'_l$  becomes ineffective; all the pairs in  $D'_l$  should be either automatically labeled by the machine or manually labeled by the human. In both cases, *r*-HUMO would merge  $D'_l$  and the rightmost uninspected unit subset adjacent to  $D_l$ ,  $D_j$ , to constitute a new candidate set,  $D_l = D'_l \cup D_j$ . It would then re-estimate pair risk based on the updated human-labeled results and begin a new pair pick-up iteration on the new  $D_l$ . To handle the case when pair selection stops too early, *r*-HUMO sets a threshold for the number of inspected pairs in each iteration.

If the number of pairs chosen for inspection is less than the threshold number, it would assign all the remaining pairs in the rightmost unit subset in the candidate set  $D_l$  to the human. The running examples of pair selection in  $D_-$  are shown in Fig. 4.

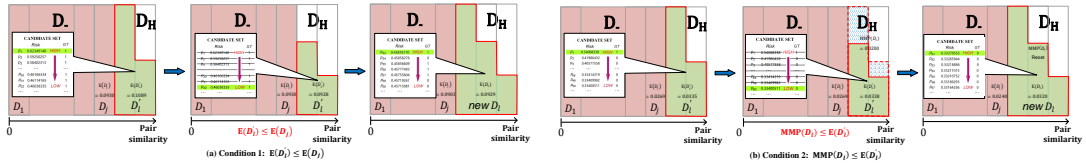


Figure 4: Running Examples of Pair Selection in  $D_-$ .

**Pair Selection in  $D_+$ .** The process of human workload selection on  $D_+$  is similar. We denote the candidate set considered for manual verification in  $D_+$  by  $D_h$ .  $r$ -HUMO iteratively selects the pairs in  $D_h$  in a risk-wise decreasing order for human verification. Note that the pairs with lower similarities are at more risk to be mislabeled by the machine. Therefore,  $D_h$  is initially set to be the leftmost unit subset in  $D_+$ , or  $D_h = D_{i+1}$  in Fig. 3. For simplicity of presentation, we denote the set of remaining pairs by  $D'_h$  and the leftmost uninspected unit subset adjacent to  $D_h$  in  $D_+$  by  $D_k$ . Iterative pair selection in  $D_h$  would stop once either one of the two following conditions is satisfied:

1. The expected match proportion of the remaining pairs in  $D'_h$  rises equal to or above the expected match proportion of the leftmost uninspected unit subset adjacent to  $D_h$  in  $D_+$ , or  $E(D'_h) \geq E(D_k)$ ;
2. The marginal match proportion of pair selection in  $D_h$ ,  $MMP(D_h)$ , rises equal to or above the expected match proportion of  $D'_h$ , or  $MMP(D_h) \geq E(D'_h)$ .

In both cases,  $r$ -HUMO would merge  $D'_h$  and  $D_k$  to constitute a new candidate set,  $D_h = D'_h \cup D_k$ . It would then re-estimate pair risk based on the updated human-labeled results and begin a new iteration of pair pick-up on the new  $D_h$ . Similar to the case of  $D_-$ ,  $r$ -HUMO sets a lower threshold for the number of inspected pairs in each iteration.

**Algorithm.** The process of human workload selection alternately selects the pairs in  $D_-$  and  $D_+$  for manual verification. Note that pair selection in  $D_-$  would elevate both precision and recall levels. In comparison, pair selection in  $D_+$  would only elevate precision level. The procedure of human workload selection is sketched in Algorithm 1. It iteratively invokes the processes of pair selection in  $D_-$  and  $D_+$  until the specified precision and recall requirements are met. Lines 4-18 specify the pair selection process in  $D_-$  and Lines 19-32 specify the pair selection process in  $D_+$ . Once the recall requirement is expected to be met, iterative pair selection in  $D_-$  would stop; more iterations of pair selection in  $D_+$  would not change the achieved recall level. Once the precision requirement is expected to be met, iterative pair selection in  $D_+$  would stop; more

iterations of pair selection in  $D_-$  could only further elevate the achieved recall level.

---

**Algorithm 1:** Human Workload Selection in  $r$ -HUMO

---

**Input:**  $D = \{D_1, D_2, \dots, D_m\}$ ,  $D_- = \{D_1, \dots, D_i\}$ ,  $D_+ = \{D_{i+1}, D_{i+2}, \dots, D_m\}$   
**Output:**  $D_H$ .

```

1  $D_l, D_h, D_H \leftarrow \emptyset;$ 
2  $j \leftarrow i, k \leftarrow (i + 1);$ 
3 while  $recall_l < \beta$  or  $precision_l < \alpha$  do
4   if  $recall_l < \beta$  then
5      $D_l \leftarrow D'_l \cap D_j;$ 
6      $j \leftarrow j - 1;$ 
7     Update  $E(D_l), E(D_j);$ 
8      $MMP(D_l)$  reset;
9     while Not ( $recall_l < \beta$  or  $E(D'_l) \leq E(D_j)$  or  $MMP(D_l) \leq E(D'_l)$ ) do
10     $p \leftarrow$  the pair with highest risk in  $D'_l;$ 
11     $D'_l \leftarrow D'_l \setminus p;$ 
12     $D_H \leftarrow p;$ 
13    Assign  $p$  for human verification;
14    Update  $E(D'_l), MMP(D_l), recall_l,$ 
15     $precision_l;$ 
16   end
17   Re-estimate pair risk;
18 end
19 if  $precision_l < \alpha$  then
20    $D_h \leftarrow D'_h \cap D_k;$ 
21    $k \leftarrow k + 1;$ 
22   Update  $E(D_h), E(D_k);$ 
23    $MMP(D_h)$  reset;
24   while Not ( $precision_l < \alpha$  or  $E(D'_h) \geq E(D_k)$  or  $MMP(D_h) \geq E(D'_h)$ ) do
25     $p \leftarrow$  the pair with highest risk in  $D'_h;$ 
26     $D'_h \leftarrow D'_h \setminus p;$ 
27     $D_H \leftarrow p;$ 
28    Assign  $p$  for human verification;
29    Update  $E(D'_h), MMP(D_h), precision_l;$ 
30   end
31   Re-estimate pair risk;
32 end
33 end
34 return  $D_H.$ 

```

---

## 4.2 QUALITY ENSURANCE

As in HUMO, the lower bounds of the achieved precision and recall levels of an  $r$ -HUMO solution are represented by Eq. 3 and Eq. 4 respectively. In this subsection, we present the

GPR process to approximate the match proportions of unit subsets and then describe how to compute the lower and upper bounds of the number of matching pairs in a given set based on GPR estimates.

**GPR Approximation.** As HUMO,  $r$ -HUMO samples a fraction of unit subsets to estimate their match proportions and then uses GPR to approximate the match proportions of other unit subsets. Suppose that  $k$  unit subsets are sampled, their observed match proportions are denoted by  $\mathbf{R} = [\mathbf{R}_1, \mathbf{R}_2, \dots, \mathbf{R}_k]^T$ , and their corresponding pair similarities by  $\mathbf{V} = [v_1, v_2, \dots, v_k]^T$ . Given a new unit subset  $D_*$  and its average pair similarity value  $v_*$ , GPR assumes that the random variables of  $[V^T, v_*]^T$  satisfy a joint Gaussian distribution, which can be represented by

$$\begin{bmatrix} V \\ v_* \end{bmatrix} \sim \mathcal{N} \left( 0, \begin{bmatrix} \mathbf{K}(V, V) & \mathbf{K}(V, v_*) \\ \mathbf{K}(v_*, V) & \mathbf{K}(v_*, v_*) \end{bmatrix} \right) \quad (7)$$

, in which  $\mathbf{K}(\cdot, \cdot)$  represents the covariance matrix. The details of how to compute the covariance matrix can be found in [35]. Based on Eq. 7, the distribution of the match proportion of  $S_*$ ,  $R_*$ , can be represented by the following Gaussian function

$$R_* \sim N(\bar{R}_*, \sigma_{R_*}^2) \quad (8)$$

, in which the mean of  $R_*$ ,  $\bar{R}_*$ , can be represented by

$$\bar{R}_* = \mathbf{K}(v_*, V) \cdot \mathbf{K}^{-1}(V, V) \cdot \mathbf{R} \quad (9)$$

, and the variance of  $R_*$ ,  $\sigma_{R_*}^2$ , can be represented by

$$\sigma_{R_*}^2 = \mathbf{K}(v_*, v_*) - \mathbf{K}(v_*, V) \cdot \mathbf{K}^{-1}(V, V) \cdot \mathbf{K}(V, v_*). \quad (10)$$

**Bound Estimation.** Provided with the Gaussian distributions of the match proportions of unit subsets, the number of matching pairs in any given set consisting of multiple unit subsets can be estimated by aggregating the distributions of unit subsets. Suppose that the pair set of  $D_*$  consists of  $t$  unit subsets,  $D_* = D_*^1 \cup D_*^2 \cup \dots \cup D_*^t$ , the total number of pairs in  $D_*^i$  ( $1 \leq i \leq t$ ) is denoted by  $n_*^i$ , and the average similarity value of the pairs in  $D_*^i$  by  $v_*^i$ . Then, the total number of matching pairs in  $D_*$ , denoted by  $m_*$ , can be represented by

$$m_* \sim N(\bar{m}_*, \sigma_{m_*}^2), \quad (11)$$

in which the mean,  $\bar{m}_*$ , can be represented by

$$\bar{m}_* = \sum_{i=1}^t n_*^i \cdot \bar{R}_*^i, \quad (12)$$

and the variance,  $\sigma_{m_*}^2$ , can be represented by

$$\sigma_{m_*}^2 = \sum_{1 \leq i \leq t, 1 \leq j \leq t} n_*^i \cdot n_*^j \cdot cov(v_*^i, v_*^j), \quad (13)$$

in which  $cov(v_*^i, v_*^j)$  is the covariance between the two estimates.

In  $r$ -HUMO, some pairs in a unit subset may be inspected by the human while others are automatically labeled by the machine. In other words,  $D_H$ ,  $D_-$  and  $D_+$  may contain a fraction of the pairs in a unit subset. Consider a pair set consisting of  $t$  subsets,  $D_*' = D_*^{1'} \cup D_*^{2'} \cup \dots \cup D_*^{t'}$ , in which  $D_*^{i'}$  denotes the set of remaining pairs in  $D_*^i$  with some of the pairs selected for manual verification and  $D_*^{i'} \neq \emptyset$ . Suppose that there are  $k$  matching pairs among all the pairs inspected by the human in  $D_*$ , or the pairs in  $D_* - D_*'$ . On the number of matching pairs in  $D_*'$ , we have the following lemma:

**Lemma 1** *Provided that the number of matching pairs in  $D_*$  can be represented by the Gaussian function of  $N(\bar{m}_*, \sigma_{m_*}^2)$ , the number of matching pairs in  $D_*'$ ,  $m_*'$ , can therefore be represented by the Gaussian function of*

$$m_*' \sim N(\bar{m}_* - k, \sigma_{m_*}^2). \quad (14)$$

**Proof 1** *Suppose that some pairs in  $D_*^i$  have been selected for manual verification and  $k_i$  pairs among them are matching pairs. The expectation of the number of matching pairs among the remaining pairs in  $D_*^i$ ,  $m_*^i'$ , can be represented by*

$$E(m_*^i') = E(m_*^i - k_i) = E(m_*^i) - k_i. \quad (15)$$

Accordingly, the expectation of the total number of matching pairs in  $D_*'$  can be represented by

$$\begin{aligned} E(m_*') &= \sum_i E(m_*^i') \\ &= \sum_i E(m_*^i) - \sum_i k_i \\ &= \bar{m}_* - k. \end{aligned} \quad (16)$$

The covariance between  $m_*^i'$  and  $m_*^j'$  can also be represented by

$$\begin{aligned} \text{cov}(m_*^i', m_*^j') &= \text{cov}(m_*^i - k_i, m_*^j - k_j) \\ &= E[(m_*^i - k_i - E(m_*^i - k_i))(m_*^j - k_j - E(m_*^j - k_j))] \\ &= E[(m_*^i - E(m_*^i))(m_*^j - E(m_*^j))] \\ &= \text{cov}(m_*^i, m_*^j). \end{aligned} \quad (17)$$

Therefore, the aggregated covariance of  $D_*'$  remains the same as that of  $D_*$ .

Note that the correctness of Lemma 1 depends on the non-emptiness of unit subsets  $D_*^i$ . If all the pairs of a unit subset have been chosen for manual inspection and it becomes empty, its estimation covariance with any other estimate on other unit subsets would become zero.

Finally, given the confidence level of  $\theta$ , the lower and upper bounds of the number of matching pairs in a subset  $D_*$  can be represented by

$$[\bar{m}_* - \mathcal{Z}_{(1-\theta)} \cdot \sigma_{m_*}, \bar{m}_* + \mathcal{Z}_{(1-\theta)} \cdot \sigma_{m_*}], \quad (18)$$

in which  $\mathcal{Z}_{(1-\theta)}$  is the  $(1 - \frac{1-\theta}{2})$  point of *standard normal distribution*.

## 5 RISK ANALYSIS

Risk analysis of  $r$ -HUMO is performed on the human-labeled results. Given a candidate pair set,  $r$ -HUMO iteratively selects the most risky pair in it for manual verification. It can be said that the performance of  $r$ -HUMO depends on the effectiveness of risk analysis. Motivated by its success in modern portfolio investment theory [36, 37, 38],  $r$ -HUMO employs the metric of Conditional Value at Risk (CVaR) to measure the risk of pairs being mislabeled by the machine.

In the portfolio risk theory, given the confidence level of  $\theta$ , CVaR is defined, in a conservative way, to be the expected loss incurred in the  $1 - \theta$  worst case. Formally, given the loss function  $z(X) \in L^p(F)$  of a portfolio  $X$  and the confidence level of  $\theta$ , the metric of CVaR is defined as

$$CVaR_\theta(X) = \frac{1}{1 - \theta} \int_0^{1-\theta} VaR_{1-\gamma}(X) d\gamma \quad (19)$$

, where  $VaR_{1-\gamma}(X)$  represents the minimum loss incurred in the  $\gamma$  worst case and can be formally represented by

$$VaR_{1-\gamma}(X) = \inf\{z_* : P(z(X) \geq z_*) \leq \gamma\}. \quad (20)$$

According to CVaR's definition, risk measurement requires the labeled pair's potential loss estimation. Intuitively, this loss refers to the probability of the pair's label being incorrect. As typical in CVaR evaluation,  $r$ -HUMO represents the match probability of a pair by a Gaussian distribution and estimates the potential loss based on it. It considers a pair as a portfolio consisting of multiple stocks. Each stock corresponds to a feature of the pair and its loss corresponds to its corresponding feature's match or unmatch probability. Note that a feature's match probability is statistically equivalent to the match proportion of the pairs containing the feature. In the rest of this section, we first describe how to extract features from human-labeled pairs, and then present the risk measurement details and analyze its complexity.

### 5.1 FEATURE EXTRACTION

For general purposes, the features used for risk analysis should have the following three desirable properties: (1) they could be easily extracted from human-labeled pairs; (2) they should be evidential, or indicative of the match status of a pair; (3) they should be independent of the machine metric used in ordering pairs in the first place. It can be observed that in  $r$ -HUMO, only the pairs in the candidate set can be chosen for manual inspection; generally, the pairs are selected into the candidate set in the order dictated by a pre-specified machine metric. Therefore, the features independent of the machine metric would be more effective than non-independent ones in differentiating pairs with similar metric values in terms of mislabeling risk.

$r$ -HUMO extracts two types of features from human-labeled pairs,  $Same(t_i)$  and  $Diff(t_i)$ , in which  $t_i$  represents a token,  $Same(t_i)$  means that  $t_i$  appears in both records in a pair, and  $Diff(t_i)$  means that  $t_i$  appears in one and only one record in a pair. It can be observed that these two features are evidential and easily extractable. Moreover, they were not used in the existing classification metrics for ER. Our risk model assumes that the match probability of

a feature satisfies a normal distribution. Given a feature  $f$  and a set of human-labeled pairs containing the feature  $f$ ,  $S_f$ , the expectation of the match probability of  $f$  can be represented by

$$E(f) = \frac{|S_f^M|}{|S_f|} \quad (21)$$

, in which  $S_f^M$  denotes the set of matching pairs in  $S_f$ . Its variance can also be represented by

$$V(f) = \frac{1}{|S_f| - 1} \sum_{p_j \in S_f} (L(p_j) - E(f))^2 \quad (22)$$

, in which  $L(p_j)$  denotes the manual label of a matching pair  $p_j$  in  $S_f$ ,  $L(p_j) = 1$  if  $p_j$  is labeled as match and  $L(p_j) = 0$  if  $p_j$  is labeled as unmatch.

## 5.2 RISK MEASUREMENT

In this subsection, we first propose the risk model for the case that features are independent; we then describe how to handle the more complicated case where the features are not independent.

According to the theory of portfolio investment, a pair's match probability distribution is the weighted linear combination of the distribution of its features. Therefore, provided with the Gaussian distributions of features, the match probability expectation of a pair  $p$ , can be represented by

$$E(p) = \sum_{f_i \in F_p} w_p(f_i) \cdot E(f_i) \quad (23)$$

, in which  $F_p$  denotes the set of features contained in  $p$ , and  $w_p(f_i)$  denotes the weight of  $f_i$  in  $p$ . Its variance can also be represented by

$$V(p) = \sum_{f_i \in F_p} w_p^2(f_i) \cdot V(f_i). \quad (24)$$

The weight of feature  $f_i$  in pair  $p$  is defined as

$$w_p(f_i) = \frac{w(f_i)}{\sum_{f_j \in F_p} w(f_j)} \quad (25)$$

, where  $w(f_i)$  denotes the absolute weight of the feature  $f_i$ .

Note that in Eq. 25, the absolute feature weights can be simply set to 1: each feature is equally powerful in predicting a given pair's match probability. In most practical scenarios, this assumption may not hold. Therefore, *r*-HUMO uses the concept of information value to determine feature weight. The metric of information value has been successfully used to estimate the predictive power of a categorical evidence or attribute in classification problems [39, 40]. *r*-HUMO regards each feature as a categorical evidence. It defines a feature  $f$ 's weight of evidence by

$$WoE(f) = \ln\left(\frac{|S_f^U|/|S_f^U|}{|S_f^M|/|S_f^M|}\right) \quad (26)$$

, in which  $S^M$  and  $S^U$  denotes the set of matching pairs and the set of unmatching pairs in human-labeled results respectively, and  $S_f^U$  denotes the set of unmatching pairs in  $S_f$ . The information value of the feature  $f$  can then be defined as

$$\begin{aligned} IV(f) &= \left( \frac{|S_f^U|}{|S^U|} - \frac{|S_f^M|}{|S^M|} \right) \cdot WoE(f) \\ &= \left( \frac{|S_f^U|}{|S^U|} - \frac{|S_f^M|}{|S^M|} \right) \cdot \ln\left(\frac{|S_f^U|/|S^U|}{|S_f^M|/|S^M|}\right). \end{aligned} \quad (27)$$

Given a pair  $p$ , we denote its match probability by  $x$ , and the probability density function and cumulative distribution function of  $x$  by  $pdf_p(x)$  and  $cdf_p(x)$  respectively. Suppose that  $p$  is originally labeled by the machine as *unmatching*. Then, the probability of  $p$  being mislabeled by the machine is equal to  $x$ . Accordingly, the worst-case loss of  $p$  corresponds to the case that  $x$  is maximal. Therefore, given the confidence level  $\theta$ , the CVaR of  $p$  is the expectation of  $z = x$  in the  $1 - \theta$  cases where  $x$  is from  $cdf_p^{-1}(\theta)$  to  $+\infty$ . Formally, the CVaR risk of a pair  $p$  with the machine label of *unmatching* can be estimated by

$$CVaR_\theta(p) = \frac{1}{1 - \theta} \int_{cdf_p^{-1}(\theta)}^{+\infty} pdf_p(x) \cdot x dx. \quad (28)$$

Otherwise,  $p$  is originally labeled by machine as *matching*. Then the potential loss of  $p$  being mislabeled by machine is equal to  $1 - x$ . Therefore, the CVaR risk of a pair  $p$  with the machine label of *matching* can be estimated by

$$CVaR_\theta(p) = \frac{1}{1 - \theta} \int_{-\infty}^{cdf_p^{-1}(1-\theta)} pdf_p(x) \cdot (1 - x) dx. \quad (29)$$

**Handling Feature Dependency.** The above-described process assumes that the extracted features are independent. However, it can be observed that this assumption may not hold true in practice. In the case that the features contained by a pair  $p$  are *not* independent, *r*-HUMO again borrows the idea of modern portfolio investment theory and introduces the covariances between features into risk measurement. We represent the variance of the match probability of a specified pair by

$$V(p) = \sum_{f_i \in F_p} \sum_{f_j \in F_p} w_p(f_i) w_p(f_j) \cdot cov(f_i, f_j). \quad (30)$$

in which  $F_p$  denotes the set of features contained in  $p$ ,  $w_p(f_i)$  denotes the weight of  $f_i$  in  $p$ , and  $cov(f_i, f_j)$  denotes the covariance between the matching probability of  $f_i$  and  $f_j$ .

Given two features  $f_i$  and  $f_j$ , their covariance,  $cov(f_i, f_j)$ , is represented by

$$E(P(M|f_i) \cdot P(M|f_j)) - E(P(M|f_i)) \cdot E(P(M|f_j)) \quad (31)$$

, in which  $P(M|f_i)$  denotes the match probability of a pair containing the feature  $f_i$ . We can estimate  $E(P(M|f_i))$  by

$$E(P(M|f_i)) = \frac{|S_{f_i}^M|}{|S_{f_i}|} \quad (32)$$

, in which  $S_{f_i}$  denotes the set of manually-labeled pairs containing the feature  $f_i$  and  $S_{f_i}^M$  denote the set of matching pairs in  $S_{f_i}$ . Similarly, we estimate  $E(P(M|f_i) \cdot P(M|f_j))$  based on the set of manually-labeled pairs containing both  $f_i$  and  $f_j$ , denoted by  $S_{(f_i, f_j)}$ , by

$$E(P(M|f_i) \cdot P(M|f_j)) = \left( \frac{|S_{(f_i, f_j)}^M|}{|S_{(f_i, f_j)}|} \right)^2 \quad (33)$$

, in which  $S_{(f_i, f_j)}^M$  denotes the set of matching pairs in  $S_{(f_i, f_j)}$ .

It can be observed that two features are correlated by co-occurrence in a pair. Accordingly,  $r$ -HUMO defines a correlation factor between two features by feature co-occurrence, and estimates their covariance if and only if their correlation factor exceeds a pre-defined threshold. We define the correlation factor between two features,  $f_i$  and  $f_j$ , by

$$CF(f_i, f_j) = \frac{P(f_i, f_j)}{P(f_i) \cdot P(f_j)} \quad (34)$$

, in which  $P(f_i)$  denotes the probability that a pair in  $D$  contains the feature of  $f_i$ , and  $P(f_i, f_j)$  the probability that a pair contains both  $f_i$  and  $f_j$ . In practical implementations, the threshold of  $CF(f_i, f_j)$  can be set between 1 and 20 (e.g. 10).

### 5.3 COMPLEXITY ANALYSIS

It can be observed that in each iteration, the total frequency of feature occurrence is bound by  $\mathcal{O}(m \cdot n)$ , in which  $n$  denotes the total number of pairs in a workload and  $m$  denotes the maximal number of tokens in a pair. As a result, the time complexity of computing feature distributions in each iteration is bounded by  $\mathcal{O}(m \cdot n)$ . Accordingly, without considering feature dependency, the time complexity of computing the CVaR risk of the candidate pairs in each iteration is also bounded by  $\mathcal{O}(m \cdot n)$ . Since the number of interactive iterations is at most  $\mathcal{O}(n)$ , the total time complexity of risk analysis can be represented by  $\mathcal{O}(m \cdot n^2)$ . Therefore, we have Theorem. 1, whose proof follows naturally from our above analysis.

**Theorem 1** *The space and time complexities of risk analysis without considering feature dependency can be represented by  $\mathcal{O}(m \cdot n)$  and  $\mathcal{O}(m \cdot n^2)$  respectively, in which  $n$  denotes the total number of pairs in a workload and  $m$  denotes the maximal number of tokens in a pair.*

Now we analyze the space and time complexity of computing feature dependency. It can be observed that the total number of pairs of interdependent features is bounded by  $\mathcal{O}(m^2 \cdot n)$ . It follows that the space complexity of computing feature dependency can be represented by  $\mathcal{O}(m^2 \cdot n)$ . The time complexity of computing their covariances is also bounded by  $\mathcal{O}(m^2 \cdot n)$ . Since feature covariances can be computed incrementally at each new iteration, the total time complexity for computing feature dependency can be represented by  $\mathcal{O}(m^2 \cdot n^2)$ .

**Proof 2** *The maximum number of human-labeled pairs and candidate pairs are the number of all pairs  $n$ , and the maximum number of iterations is also  $n$  when extreme case occurs that r-HUMO updates risk model every pair verification and assigns all the pairs for human verification. Assuming that the maximum number of tokens contained in an entity record is constant*

$c$ , then the maximum number of human labeled results as samples of all the features is  $2c \cdot n$  in total: Consider that we have assigns all the  $n$  pairs for human verification; if there are no same features between any 2 pairs, then each feature will have only 1 sampled result, and the total number of these results is  $1 \cdot 2c \cdot n = 2c \cdot n$ ; once there is a feature appears 1 time more among these pairs, the feature will have 1 more sampled results, while the number of total different features of the pairs will decrease 1, therefore, the number of human labeled results of all the features stays the same as  $2c \cdot n$ ; and so on, the maximum number of human labeled results of all the features always keeps  $2c \cdot n$  in total.

The time complexity of r-HUMO consists of computing on many iterations, and for each iteration, the computing mainly consists of 2 parts: (1) the estimation of expectations and variances of the distributions of features, taking  $O(2c \cdot n) = O(n)$  time on processing the human labeled results of all the features; (2) the estimation of risks of candidate pairs, taking  $2c \cdot O(n) = O(n)$  time on processing the distributions of all candidate pairs; (3) sorting the candidate pairs in the decreasing order of risk, taking  $O(n \cdot \log(n))$  time. Therefore, for  $n$  iterations, the time complexity of r-HUMO is  $O(n^2 \cdot \log(n))$ .

The space complexity of r-HUMO consists of storage mainly consists of 2 parts: (1) the features and their expectations and variances of the distributions; (2) the candidate pairs and their risks. Each part needs  $O(n)$  space. Therefore, the space complexity of r-HUMO is  $O(n)$ .

## 6 EXPERIMENTAL STUDY

In this section, we empirically evaluate the performance of *r*-HUMO on real datasets by comparative study. We compare *r*-HUMO with the state-of-the-art alternative HUMO [14, 15], which can enforce both precision and recall. *Note that most of existing ER techniques can not enforce the quality guarantees measured by precision and recall. The performance difference between these techniques is beyond the scope of this paper.* Additionally, we compare *r*-HUMO with the active learning-based approach (denoted by ACTL) [12], which can at least enforce precision. ACTL can maximize recall while ensuring a pre-specified precision level. It estimates the achieved precision level of a labeling solution by sampling. As a result, ACTL also requires manual verification. We compare *r*-HUMO with ACTL on their achieved qualities and required manual costs.

The rest of this section is organized as follows: Subsection. 6.1 describes the experimental setup. Subsection. 6.2 presents the quality enforcement results of *r*-HUMO. Subsection. 6.3 compares the performance of *r*-HUMO with that of HUMO on required manual cost given the same quality requirements. Subsection. 6.4 compares the performance of *r*-HUMO with that of ACTL on achieved quality and required manual cost. Subsection. 6.5 evaluates the effectiveness of the proposed risk model. Subsection. 6.6 evaluates the effectiveness of feature weighting in risk measurement. Subsection. 6.7 evaluates the effect of handling feature dependency. Finally, Subsection. 6.8 evaluates the efficiency and scalability of *r*-HUMO.

In this section, we empirically evaluate the performance of *r*-HUMO on real datasets by comparative study. We compare *r*-HUMO with the state-of-the-art alternative HUMO [14, 15], which can enforce both precision and recall. *Note that most of existing ER techniques can not enforce the quality guarantees measured by precision and recall. The performance difference between these techniques is beyond the scope of this paper.*

between these techniques is beyond the scope of this paper. Additionally, we compare *r*-HUMO with the active learning-based approach (denoted by ACTL) [12], which can at least enforce precision. ACTL can maximize recall while ensuring a pre-specified precision level. It estimates the achieved precision level of a labeling solution by sampling. As a result, ACTL also requires manual verification. We compare *r*-HUMO with ACTL on the achieved quality and the required manual cost.

The rest of this section is organized as follows: Subsection 6.1 describes the experimental setup. Subsection 6.2 presents the quality enforcement results of *r*-HUMO. Subsection 6.3 compares the performance of *r*-HUMO with that of HUMO. Subsection 6.4 compares the performance of *r*-HUMO with that of ACTL. Subsection 6.6 evaluates the effectiveness of feature weighting in risk measurement. Finally, Subsection 6.8 evaluates the efficiency and scalability of *r*-HUMO.

## 6.1 EXPERIMENTAL SETUP

Our evaluation is conducted on the three real datasets, whose details are described as follows:

- DBLP-Scholar<sup>1</sup> (denoted by DS): The DS dataset contains 2616 publication entities from DBLP publications and 64263 publication entities from Google Scholar. The experiments match the DBLP entries with the Scholar entries.
- Abt-Buy<sup>2</sup> (denoted by AB): The AB dataset contains 1081 product entities from Abt.com and 1092 product entities from Buy.com. The experiments match the Abt entries with the Buy entries.
- Songs<sup>3</sup> (denoted by SG): The SG dataset contains 1000000 songs entities, some of which refer to the same songs. The experiments match the songs entries in the same table.

Our empirical study uses pair similarity as the machine metric. It computes pair similarity by aggregating attribute similarities with weights [14, 15]. Specifically, on the DS dataset, Jaccard similarity of the attributes *title* and *authors*, and Jaro-Winkler distance of the attribute *venue* are used; on the AB dataset, Jaccard similarity of the attributes *product name* and *product description* are used; on the SG dataset, Jaccard similarity of the attributes *song title*, *release information* and *artist name*, Jaro-Winkler distance of the attributes *song title* and *release information*, and number similarity of the attributes *duration*, *artist familiarity*, *artist hotness* and *year* are used. The weight of each attribute is determined by the number of its distinct attribute values. As in [12, 14], we use the blocking technique to filter the instance pairs unlikely to match. Specifically, the DS workload contains the instance pairs whose aggregated similarity values are no less than 0.2. Similarly, the aggregated similarity value thresholds for the AB and SG workloads are set to 0.05 and 0.2. After blocking, the DS workload has 100077 pairs, 5267 among them are matching pairs; the AB workload has 313040 pairs, 1085 among them are matching pairs; the SG workload has 289893 pairs and 13756 among them are matching pairs.

---

<sup>1</sup>available at <https://dbs.uni-leipzig.de/file/DBLP-Scholar.zip>

<sup>2</sup>available at <https://dbs.uni-leipzig.de/file/Abt-Buy.zip>

<sup>3</sup>available at [http://pages.cs.wisc.edu/~anhai/data/falcon\\_data/songs](http://pages.cs.wisc.edu/~anhai/data/falcon_data/songs)

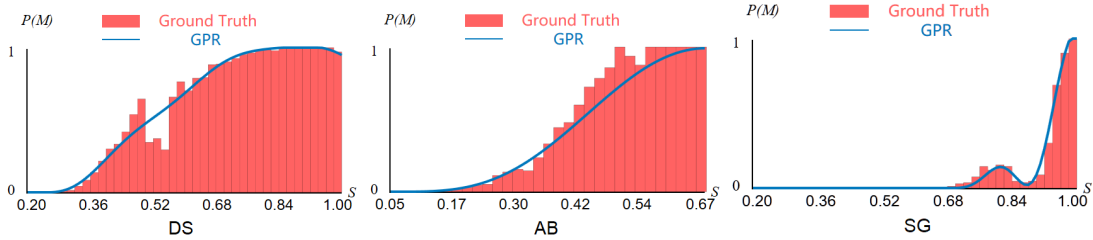


Figure 5: the Match Proportions of Subsets with regard to Pair Similarity.

As in the HUMO implementation, our  $r$ -HUMO implementation partitions an ER workload into disjoint subsets, each of which contains the same number of instance pairs. The number of instance pairs contained by each subset is set to 200. The match proportions of the subsets with regard to pair similarity on the three workloads are presented in Figure. 5, in which the X-axis represents pair similarity value and the Y-axis represents the match proportion. It can be observed that all the three workloads roughly but not strictly satisfy the monotonicity assumption of precision, and SG violates the monotonicity assumption to the greatest extent among the three workloads.

To balance the sampling cost and accuracy of match proportion approximation, as in the HUMO implementation [14],  $r$ -HUMO sets both lower and upper limits on sampling cost, which is measured by the proportion of sampled subsets among all the subsets. In our experiments, the range of the sampling proportion is set between 3% and 5%. We observe that considering feature dependency in risk analysis for  $r$ -HUMO can only marginally improve the performance on the test workloads. We report both the results of  $r$ -HUMO without considering feature dependency and considering feature dependency in this technical report.

Note that in  $r$ -HUMO, different runs may generate different labeling solutions due to sampling randomness. For each experiment, we therefore run the program 20 times on each workload and report the averaged result. In our experiments, we have the ground-truth labels of all the test pairs. The ground-truth labels are originally hidden; whenever manual verification is called, they are provided to the program. Existing crowdsourcing platforms can obviously be used to perform manual verification. Integrating HUMO with the crowdsourcing platforms is an interesting future work. It is however beyond the scope of this paper.

## 6.2 QUALITY ENFORCEMENT

In our experiments, we specify 7 scales of quality requirement, whose precision and recall are set at different levels at 0.8, 0.825, 0.85, 0.875, 0.9, 0.925 and 0.95 respectively. The confidence level on the quality guarantee is set at 0.9.

Table 1: Quality Enforcement

Dataset	Required Quality $\alpha=\beta$	Achieved Quality		
		$\alpha$	$\beta$	SR(%)
DS	0.825	0.9079	0.8459	100
	0.850	0.9098	0.8657	100
	0.875	0.9124	0.8904	100
	0.900	0.9248	0.9150	100
	0.925	0.9497	0.9391	100
	0.950	0.9748	0.9628	95
AB	0.800	0.9629	0.8546	100
	0.825	0.9630	0.8589	100
	0.850	0.9635	0.8718	100
	0.875	0.9643	0.8920	100
	0.900	0.9651	0.9112	100
	0.925	0.9671	0.9398	100
	0.950	0.9693	0.9508	90
SG	0.800	0.9663	0.8957	90
	0.825	0.9671	0.9201	90
	0.850	0.9678	0.9417	90
	0.875	0.9683	0.9581	90
	0.900	0.9686	0.9660	90
	0.925	0.9687	0.9694	90
	0.950	0.9746	0.9708	90

The detailed evaluation results on the DS, AB and SG datasets are presented in Table 1, in which  $\alpha$  denotes precision,  $\beta$  denotes recall, and  $SR$  denotes success rate, which represents the percentage of the successful runs achieving required quality levels among all the runs. Note that on DS, the initial machine labeling solution achieves precision and recall levels above 0.8; we therefore do not report its results in the table. It can be observed that  $r$ -HUMO is effective in ensuring quality guarantees. On all the three workloads, the achieved quality levels are considerably above the required levels in most cases and the achieved success rates consistently exceed the confidence level of 0.9.

### 6.3 $r$ -HUMO vs HUMO

We compare the manual cost consumed by  $r$ -HUMO and HUMO given the same quality requirements. Bear in mind that the manual cost includes both the sampling cost and the cost of manually inspecting the pairs in  $D_H$ . Since  $r$ -HUMO and HUMO consume the same amount of sampling cost in each run, we compare the sizes of their resulting pair set requiring manual inspection (excluding sampled pairs),  $D_H$ . On all the three datasets, the consumed sampling cost is very close to the upper limit of 5% in most runs; averagely, the sampling cost of the DS, AB and SG datasets are 4.93%, 4.94% and 4.96% respectively.

The comparative results of  $r$ -HUMO and HUMO on the three workloads are presented in

Table 2. It can be observed that given the same quality requirement,  $r$ -HUMO consistently outperforms HUMO and their performance margin is considerable in most cases. In general,  $r$ -HUMO's performance advantage over HUMO decreases with the escalating quality requirement. These observations clearly validate the effectiveness of  $r$ -HUMO's risk analysis-based pair prioritization strategy.

Table 2: Performance Comparison between  $r$ -HUMO and HUMO

Data set	Required Quality $\alpha=\beta$	Size of $D_H$ (excl. samples)		
		HUMO	$r$ -HUMO	Reduction(%)
DS	0.825	108	<b>37</b>	65.74
	0.850	463	<b>151</b>	67.39
	0.875	927	<b>302</b>	67.42
	0.900	1255	<b>538</b>	57.13
	0.925	1852	<b>967</b>	47.79
	0.950	2802	<b>1786</b>	36.26
AB	0.800	4628	<b>4144</b>	10.46
	0.825	6056	<b>5664</b>	6.47
	0.850	7894	<b>7179</b>	9.06
	0.875	10239	<b>8328</b>	18.66
	0.900	13495	<b>10662</b>	20.99
	0.925	28273	<b>27380</b>	3.16
	0.950	34649	<b>34136</b>	1.48
SG	0.800	62940	<b>28007</b>	55.50
	0.825	66672	<b>34615</b>	48.08
	0.850	68598	<b>43055</b>	37.24
	0.875	71667	<b>59654</b>	16.76
	0.900	75698	<b>74156</b>	2.04
	0.925	83156	<b>81903</b>	1.51
	0.950	89742	<b>88190</b>	1.73

The results reported above are based on the GPR approximations that use samples, which consists of only a small portion (less than 5%) of all the pairs in a workload. However, the GPR approximations based on samples may not be accurate in many instances. The estimation inaccuracies resulting from GPR approximation may significantly affect the computation of  $D_H$ 's boundaries. To further validate the effectiveness of  $r$ -HUMO's pair prioritization strategy, we also execute  $r$ -HUMO and HUMO with the assumption that the estimations of subset match proportions are accurate. In the new experimental setting, both  $r$ -HUMO and HUMO are given the exact number of matching pairs in each subset (instead of GPR estimation) beforehand as well as the same quality requirement. The comparative results on the three workloads are presented in Table 3. It can be observed that  $r$ -HUMO consistently outperforms HUMO in all the test cases, and compared with the previous GPR approximation setting,  $r$ -HUMO outperforms it by more considerable margins. *Even though the results reported in Table 3 are not realistic in practical scenarios, they do illustrate the efficacy of  $r$ -HUMO's pair prioritization strategy*

and demonstrate that the performance advantage of  $r$ -HUMO over HUMO can increase with the accuracy of GPR approximation.

Table 3: Performance Comparison between  $r$ -HUMO and HUMO with Ground-Truth Match Proportions

Data set	Required Quality $\alpha=\beta$	Size of $D_H$ (excl. samples)		
		HUMO	$r$ -HUMO	Reduction(%)
DS	0.850	443	<b>78</b>	82.39
	0.875	949	<b>221</b>	76.71
	0.900	1080	<b>373</b>	65.46
	0.925	1574	<b>586</b>	62.77
	0.950	2545	<b>1020</b>	59.92
AB	0.800	2519	<b>953</b>	62.17
	0.825	3997	<b>1359</b>	66.00
	0.850	5971	<b>2041</b>	65.82
	0.875	9617	<b>2899</b>	69.86
	0.900	12671	<b>4045</b>	68.08
	0.925	19466	<b>14628</b>	24.85
	0.950	33226	<b>32020</b>	3.77
SG	0.800	62298	<b>12796</b>	79.46
	0.825	65101	<b>14052</b>	78.42
	0.850	67983	<b>15505</b>	77.19
	0.875	71006	<b>17558</b>	75.27
	0.900	72820	<b>19584</b>	73.11
	0.925	75640	<b>23693</b>	68.68
	0.950	80869	<b>30287</b>	62.55

## 6.4 $r$ -HUMO vs ACTL

Table 4: Comparison between  $r$ -HUMO and ACTL on Recall given the Same Precision.

Data set	Required Precision	Achieved Recall		$\psi(\%)$		$\frac{\Delta\psi}{100 \cdot \Delta Recall}$
		$r$ -HUMO	ACTL	$r$ -HUMO	ACTL	
DS	0.825	0.8459	0.8176	4.97	3.46	0.5335
	0.850	0.8657	0.7999	5.08	3.70	0.2097
	0.875	0.8904	0.8000	5.23	2.98	0.2489
	0.900	0.9150	0.7662	5.47	3.17	0.1546
	0.925	0.9391	0.7557	5.90	3.83	0.1129
	0.950	0.9628	0.7273	6.71	2.56	0.1762
AB	0.800	0.8546	0.1558	6.26	0.29	0.0854
	0.825	0.8589	0.1395	6.75	0.28	0.0899
	0.850	0.8718	0.1578	7.23	0.28	0.0973
	0.875	0.8920	0.1152	7.60	0.27	0.0944
	0.900	0.9112	0.1152	8.35	0.29	0.1013
	0.925	0.9398	0.0857	13.69	0.19	0.1581
	0.950	0.9508	0.0857	15.85	0.19	0.1810
SG	0.800	0.8957	0.3337	14.62	0.30	0.2548
	0.825	0.9201	0.3284	16.90	0.27	0.2811
	0.850	0.9417	0.3271	19.81	0.34	0.3168
	0.875	0.9581	0.3259	25.54	0.42	0.3973
	0.900	0.9660	0.3107	30.54	0.54	0.4578
	0.925	0.9694	0.2530	33.21	0.42	0.4577
	0.950	0.9708	0.2469	35.38	0.38	0.4835

In this subsection, we compare  $r$ -HUMO with the active learning based (ACTL) alternative. We have implemented of both of the techniques proposed in [12] and [13] respectively. Our experiments showed that they perform similarly on the achieved quality and required manual work. Here, we present the comparative evaluation results between  $r$ -HUMO and the technique proposed in [12]. As [12], we employ Jaccard similarity, edit distance and number similarity on attributes used in Subsection 6.1 as the similarity space for ACTL. On DS, the used attributes are *title* and *authors*; on AB, they are *product name* and *product description*; and on SG, they are *song title*, *release information*, *artist name*, *duration*, *artist familiarity*, *artist hotness* and *year*. ACTL uses sampling to estimate the achieved precision level of a given classification solution; therefore it also requires manual work.

In our experiments, the required precision and recall levels are set to be the same for  $r$ -HUMO. Considering that ACTL can not enforce recall level; at each given precision level, we record  $r$ -HUMO and ACTL's differences on the achieved recall and the consumed human cost. The performance comparisons between  $r$ -HUMO and ACTL are presented in Table 4, in which  $\psi$  represents the percentage of manual work, and  $\Delta$  denotes the performance difference between the two methods on a specified metric. It can be observed that the achieved recall level by ACTL

generally decreases with the specified precision level. In all the test cases,  $r$ -HUMO achieves higher recall levels than ACTL. We also record the additional human cost required by  $r$ -HUMO for the absolute recall improvement of 1% over ACTL (at the last columns of Table 4. It can be observed that, with both precision and recall set at the high level of 0.95, the cost is as low as 0.1762% on DS, 0.1810% on AB and 0.4835% on SG.

Table 5: Comparison between  $r$ -HUMO and ACTL on F1 given the Same Precision.

Data set	Required Precision	Achieved F1		$\psi(\%)$		$\frac{\Delta\psi}{100 \cdot \Delta F1}$
		$r$ -HUMO	ACTL	$r$ -HUMO	ACTL	
DS	0.825	0.8758	0.8057	4.97	3.46	0.2154
	0.850	0.8872	0.8067	5.08	3.70	0.1714
	0.875	0.9013	0.8130	5.23	2.98	0.2548
	0.900	0.9199	0.8187	5.47	3.17	0.2273
	0.925	0.9444	0.8220	5.90	3.83	0.1691
	0.950	0.9688	0.8161	6.71	2.56	0.2718
AB	0.800	0.9055	0.2626	6.26	0.29	0.0929
	0.825	0.9080	0.2408	6.75	0.28	0.0970
	0.850	0.9154	0.2653	7.23	0.28	0.1069
	0.875	0.9267	0.2053	7.60	0.27	0.1016
	0.900	0.9374	0.2053	8.35	0.29	0.1101
	0.925	0.9533	0.1575	13.69	0.19	0.1696
	0.950	0.9600	0.1575	15.85	0.19	0.1951
	0.800	0.9297	0.4807	14.62	0.30	0.3189
SG	0.825	0.9430	0.4790	16.90	0.27	0.3584
	0.850	0.9546	0.4780	19.81	0.34	0.4085
	0.875	0.9632	0.4769	25.54	0.42	0.5166
	0.900	0.9673	0.4629	30.54	0.54	0.5948
	0.925	0.9690	0.4013	33.21	0.42	0.5776
	0.950	0.9727	0.3939	35.38	0.38	0.6047

It can be observed that given the same precision requirement, ACTL and  $r$ -HUMO might actually achieve different precision levels. Therefore, we also compare their actual performance on the F1 metric and record the additional human cost required by  $r$ -HUMO for the absolute F1 improvement of 1% over ACTL. The detailed results are presented in Table 5. Similar to what was observed in Table 4, the additional human cost generally increases with the specified precision level. On DS, the additional human cost of  $r$ -HUMO for 1% increase in F1 score is maxed at 0.2718%. On AB and SG, it is as low as 0.1951% and 0.6047% respectively. Along with the results presented in Table 4, these results clearly demonstrate that compared with ACTL,  $r$ -HUMO can effectively improve the resolution quality with reasonable ROI in terms of human cost.

## 6.5 RISK MODEL EFFECTIVENESS

In order to evaluate the effectiveness of the CVaR risk model proposed for  $r$ -HUMO, we compare its performance to that of the expectation loss (EL) risk model in this subsection. The EL model simply computes the mislabeled risk of a pair as the expectation of its mislabeled probability. Therefore, the EL model estimates the risk of a pair  $p$  with the machine label of *unmatching* as

$$EL(p) = E(x) \quad (35)$$

, and the risk of a pair  $p$  with the machine label of *matching* as

$$EL(p) = 1 - E(x) \quad (36)$$

, where  $E(x)$  stands for the estimated probability expectation of  $p$  being matching based on feature distributions.

Table 6: Risk Model Evaluation

Dataset	Required Quality $\alpha=\beta$	Size of $D_H$ (excl. samples)	
		EL	CVaR
DS	0.825	<b>49</b>	<b>49</b>
	0.850	<b>177</b>	<b>177</b>
	0.875	357	<b>353</b>
	0.900	656	<b>646</b>
	0.925	1208	<b>1200</b>
	0.950	2320	<b>2319</b>
AB	0.800	4080	<b>4062</b>
	0.825	5620	<b>5361</b>
	0.850	7330	<b>7326</b>
	0.875	9533	<b>9365</b>
	0.900	11675	<b>10716</b>
	0.925	<b>27378</b>	27380
	0.950	<b>34124</b>	34136
SG	0.800	29603	<b>28007</b>
	0.825	37036	<b>34615</b>
	0.850	46462	<b>43055</b>
	0.875	62291	<b>59654</b>
	0.900	76462	<b>74156</b>
	0.925	84050	<b>81903</b>
	0.950	89710	<b>88190</b>

Table 7: Risk Model Evaluation with Ground-Truth Match Proportions

Dataset	Required Quality $\alpha=\beta$	Size of $D_H$ (excl. samples)	
		EL	CVaR
DS	0.850	69	<b>68</b>
	0.875	<b>210</b>	<b>210</b>
	0.900	372	<b>367</b>
	0.925	588	<b>577</b>
	0.950	1027	<b>1018</b>
AB	0.800	1375	<b>1246</b>
	0.825	2006	<b>1824</b>
	0.850	2958	<b>2681</b>
	0.875	3795	<b>3683</b>
	0.900	5078	<b>5066</b>
	0.925	18753	<b>16739</b>
	0.950	<b>31845</b>	31863
SG	0.800	12978	<b>12796</b>
	0.825	14324	<b>14052</b>
	0.850	16033	<b>15505</b>
	0.875	18513	<b>17558</b>
	0.900	20826	<b>19584</b>
	0.925	26571	<b>23693</b>
	0.950	36577	<b>30287</b>

The comparative results of the CVaR and EL risk models on the three workloads are presented in Table 6. Their comparative performance provided with ground-truth match proportions are also presented in Table 7. In all the tables, the cost corresponding to the better performance is emphasized in **bold**. It can be observed that given the same quality requirement, the CVaR risk model requires less human cost than the EL model on most of the test cases (in the cases of SG, the margins are considerable); in the cases where it performs worse, their cost difference is only marginal. EL selects pairs on their incorrect probability on average, while CVaR remains risk-averse to select pairs based on the cases that are most probable to be incorrect. Our experimental results show that for the complicated and challenging ER workloads, a pair is usually not “lucky” enough to be correctly labeled by chance on some optimistic cases, and even not on average. It is thus sensible that we remain conservative and critical, to consider the target pairs with a more prudent care on those worst cases that could occur with a certain probability.

## 6.6 EFFECTIVENESS OF FEATURE WEIGHTING

Table 8: Evaluation of Feature Weighting

Dataset	Required Quality $\alpha=\beta$	Size of $D_H$ (excl. samples)	
		EW	IV
DS	0.825	<b>37</b>	<b>37</b>
	0.850	152	<b>151</b>
	0.875	303	<b>302</b>
	0.900	540	<b>538</b>
	0.925	980	<b>967</b>
	0.950	1817	<b>1786</b>
AB	0.800	4465	<b>4144</b>
	0.825	5714	<b>5664</b>
	0.850	7586	<b>7179</b>
	0.875	9085	<b>8328</b>
	0.900	11403	<b>10662</b>
	0.925	27403	<b>27380</b>
	0.950	34159	<b>34136</b>
SG	0.800	25230	<b>19062</b>
	0.825	26920	<b>20587</b>
	0.850	29480	<b>22807</b>
	0.875	33604	<b>26025</b>
	0.900	35126	<b>30470</b>
	0.925	43277	<b>36368</b>
	0.950	82078	<b>81603</b>

In this subsection, we evaluate the effectiveness of  $r$ -HUMO’s feature weighting strategy based on information value (IV). We compare it with the simple equally-weighting alternative (EW). The comparative results on the three workloads are presented in Table 8. Their comparative performance provided with ground-truth match proportions are also presented in Table 9. It is clear that IV consistently outperforms EW, and in some cases, their performance margins are significant. Our experimental results demonstrate the effectiveness of the feature weighting strategy based on information value.

Table 9: Evaluation of Feature Weighting with Ground-Truth Match Proportions

Dataset	Required Quality	Size of $D_H$ (excl. samples)	
	$\alpha=\beta$	EW	IV
DS	0.850	<b>78</b>	<b>78</b>
	0.875	<b>221</b>	<b>221</b>
	0.900	376	<b>373</b>
	0.925	591	<b>586</b>
	0.950	1026	<b>1020</b>
AB	0.800	1222	<b>953</b>
	0.825	1921	<b>1359</b>
	0.850	2911	<b>2041</b>
	0.875	4082	<b>2899</b>
	0.900	7067	<b>4045</b>
	0.925	17940	<b>14628</b>
	0.950	32025	<b>32020</b>
SG	0.800	13494	<b>12796</b>
	0.825	14801	<b>14052</b>
	0.850	16318	<b>15505</b>
	0.875	18553	<b>17558</b>
	0.900	20655	<b>19584</b>
	0.925	24754	<b>23693</b>
	0.950	32138	<b>30287</b>

## 6.7 EVALUATION OF CONSIDERING FEATURE DEPENDENCY

In this subsection, we evaluate the effect of handling feature dependency. We detect the correlated features by their correlation factors  $CF$ , and involve their covariances into pairs' match distribution estimation and risk measurement. The human verification costs of considering feature dependency (denoted by  $FD$ ) compared to the costs without considering feature dependency (denoted by  $FI$ ) are presented in Table 10, and their comparative performance provided with ground-truth match proportions are also presented in Table 11. Note that it is hard to accurately obtain the correlation factor and covariances between different features with limited pairs and samples, therefore, the improvements on most test cases are marginal.

Table 10: Evaluation of Considering Feature Dependency

Dataset	Required Quality $\alpha=\beta$	Size of $D_H$ (excl. samples)	
		FI	FD
DS	0.825	<b>36</b>	35
	0.850	<b>167</b>	<b>167</b>
	0.875	313	<b>312</b>
	0.900	541	<b>543</b>
	0.925	<b>1002</b>	1011
	0.950	2296	<b>2212</b>
AB	0.800	3771	<b>3752</b>
	0.825	4943	<b>4983</b>
	0.850	6741	<b>6734</b>
	0.875	9234	<b>9157</b>
	0.900	11213	<b>11112</b>
	0.925	<b>26172</b>	<b>26172</b>
	0.950	<b>35155</b>	<b>35155</b>
SG	0.800	28007	<b>27220</b>
	0.825	34615	<b>33805</b>
	0.850	43055	<b>42690</b>
	0.875	59654	<b>59205</b>
	0.900	74156	<b>73709</b>
	0.925	<b>81903</b>	81966
	0.950	<b>88190</b>	88299

Table 11: Evaluation of Considering Feature Dependency with Ground-Truth Match Proportions

Dataset	Required Quality	Size of $D_H$ (excl. samples)	
	$\alpha=\beta$	FI	FD
DS	0.850	<b>67</b>	<b>67</b>
	0.875	<b>209</b>	<b>209</b>
	0.900	<b>365</b>	<b>365</b>
	0.925	<b>575</b>	<b>575</b>
	0.950	1020	<b>1019</b>
AB	0.800	1180	<b>1206</b>
	0.825	<b>1759</b>	1787
	0.850	2630	<b>2620</b>
	0.875	<b>3667</b>	3674
	0.900	5105	<b>5033</b>
	0.925	<b>13728</b>	13750
	0.950	<b>31866</b>	31871
SG	0.800	12796	<b>12741</b>
	0.825	14052	<b>13895</b>
	0.850	15505	<b>15339</b>
	0.875	17558	<b>17167</b>
	0.900	19584	<b>19049</b>
	0.925	23693	<b>23555</b>
	0.950	30287	<b>30052</b>

## 6.8 EFFICIENCY AND SCALABILITY

In this subsection, we evaluate the efficiency and scalability of our  $r$ -HUMO implementation on different data scales. We perform random sampling on the DS dataset to generate the test workloads with different data scales. We measure the efficiency by the consumed run time.

The evaluation results are presented in Figure 6. It can be observed that as data scale increases, the run time increases polynomially as dictated by the complexity analysis results. As expected, the run time increases more dramatically with data scale as the quality requirement becomes more strict.

## 7 CONCLUSION

In this paper, we have proposed a risk-aware human-machine cooperation framework,  $r$ -HUMO, for entity resolution with quality guarantees. Different from the existing HUMO framework,  $r$ -HUMO takes advantage of the manually-labeled results to measure the risk of pairs being mislabeled by machine, thus can effectively reduce required manual work. Our extensive experiments on real data have also validated the efficacy of  $r$ -HUMO.

For large workload, crowdsourcing may be the only feasible solution for human verification. It is interesting to integrate  $r$ -HUMO into the existing crowdsourcing platforms in future work.

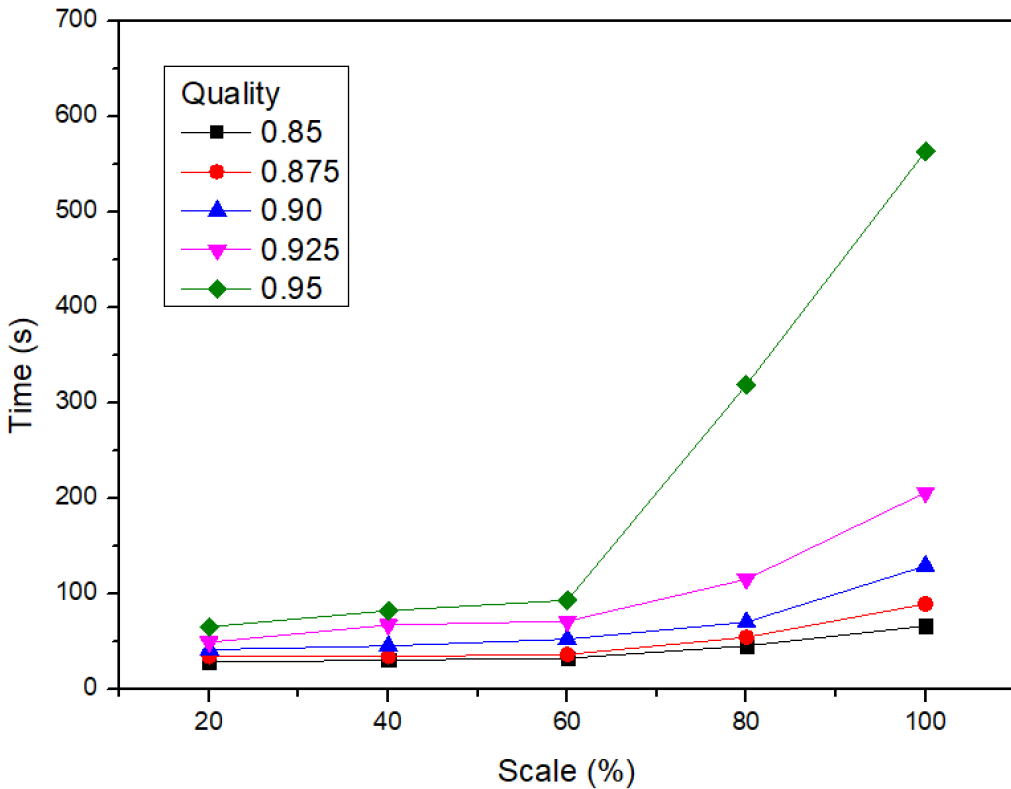


Figure 6: *r*-HUMO Efficiency and Scalability on DS.

On the crowdsourcing platforms, monetary cost may be a more appropriate metric of human cost than the number of manually inspected pairs used in this paper.

## REFERENCES

- [1] P. Christen, “*Data matching: concepts and techniques for record linkage, entity resolution, and duplicate detection*,” Springer Publishing Company, Incorporated, 2012.
- [2] A. K. Elmagarmid, P. G. Ipeirotis, and V. S. Verykios, “*Duplicate record detection: A survey*,” IEEE Transactions on Knowledge and Data Engineering, vol. 19, no. 1, pp. 1–16, 2007.
- [3] I. P. Fellegi and A. B. Sunter, “*A theory for record linkage*,” Journal of the American Statistical Association, vol. 64, no. 328, pp. 1183–1210, 1969.
- [4] W. Fan, X. Jia, J. Li, and S. Ma, “*Reasoning about record matching rules*,” Proceedings of the VLDB Endowment, vol. 2, no. 1, pp. 407–418, 2009.

[5] *L. Li, J. Li, and H. Gao, “Rule-based method for entity resolution,” IEEE Transactions On Knowledge And Data Engineering, vol. 27, no. 1, pp. 250–263, 2015.*

[6] *R. Singh, V. Meduri, A. Elmagarmid, S. Madden, P. Papotti, J.-A. Quiané-Ruiz, A. Solar-Lezama, and N. Tang, “Generating concise entity matching rules,” in Proceedings of the ACM International Conference on Management of data (SIGMOD), pp. 1635–1638, 2017.*

[7] *S. Sarawagi and A. Bhamidipaty, “Interactive deduplication using active learning,” in Proceedings of the ACM International Conference on Knowledge Discovery and Data Mining (SIGKDD), pp. 269–278, ACM, 2002.*

[8] *P. Christen, “Automatic record linkage using seeded nearest neighbour and support vector machine classification,” in Proceedings of the ACM International Conference on Knowledge Discovery and Data Mining (SIGKDD), pp. 151–159, ACM, 2008.*

[9] *B. Mozafari, P. Sarkar, M. Franklin, M. Jordan, and S. Madden, “Scaling up crowdsourcing to very large datasets: a case for active learning,” Proceedings of the VLDB Endowment, vol. 8, no. 2, pp. 125–136, 2014.*

[10] *G. Li, “Human-in-the-loop data integration,” Proceedings of the VLDB Endowment, vol. 10, no. 12, pp. 2006–2017, 2017.*

[11] *Y. Zhuang, G. Li, Z. Zhong, and J. Feng, “Hike: A hybrid human-machine method for entity alignment in large-scale knowledge bases,” in Proceedings of ACM Conference on Information and Knowledge Management (CIKM), pp. 1917–1926, 2017.*

[12] *A. Arasu, M. Götz, and R. Kaushik, “On active learning of record matching packages,” in Proceedings of the ACM International Conference on Management of data (SIGMOD), pp. 783–794, 2010.*

[13] *K. Bellare, S. Iyengar, A. G. Parameswaran, and V. Rastogi, “Active sampling for entity matching,” in Proceedings of the ACM International Conference on Knowledge Discovery and Data Mining (SIGKDD), pp. 1131–1139, 2012.*

[14] *Z. Chen, Q. Chen, and Z. Li, “A human-and-machine cooperative framework for entity resolution with quality guarantees,” Proceedings of the IEEE 33rd International Conference on Data Engineering (ICDE), Demo paper, pp. 1405–1406, 2017.*

[15] *Z. Chen, Q. Chen, F. Fan, Y. Wang, Z. Wang, Y. Nafa, Z. Li, H. Liu, and W. Pan, “Enabling quality control for entity resolution: A human and machine cooperation framework,” IEEE 34th International Conference on Data Engineering (ICDE), 2018.*

[16] *C. Chai, G. Li, J. Li, D. Deng, and J. Feng, “Cost-effective crowdsourced entity resolution: A partial-order approach,” Proceedings of the ACM International Conference on Management of Data (SIGMOD), pp. 969–984, 2016.*

[17] *G. Li, J. Wang, Y. Zheng, and M. J. Franklin, “Crowdsourced data management: A survey,” IEEE Transactions on Knowledge and Data Engineering, vol. 28, no. 9, pp. 2296–2319, 2016.*

[18] J. Wang, T. Kraska, M. J. Franklin, and J. Feng, “*Crowder: Crowdsourcing entity resolution*,” Proceedings of the VLDB Endowment, vol. 5, no. 11, pp. 1483–1494, 2012.

[19] N. Vesdapunt, K. Bellare, and N. Dalvi, “*Crowdsourcing algorithms for entity resolution*,” Proceedings of the VLDB Endowment, vol. 7, no. 12, pp. 1071–1082, 2014.

[20] P. Singla and P. Domingos, “*Entity resolution with markov logic*,” IEEE 6th International Conference on Data Mining (ICDM), pp. 572–582, 2006.

[21] S. E. Whang, D. Marmaros, and H. Garcia-Molina, “*Pay-as-you-go entity resolution*,” IEEE Transactions on Knowledge and Data Engineering, vol. 25, no. 5, pp. 1111–1124, 2013.

[22] Y. Altowim, D. V. Kalashnikov, and S. Mehrotra, “*Progressive approach to relational entity resolution*,” Proceedings of the VLDB Endowment, vol. 7, no. 11, pp. 999–1010, 2014.

[23] S. Lacoste-Julien, K. Palla, A. Davies, G. Kasneci, T. Graepel, and Z. Ghahramani, “*Sigma: Simple greedy matching for aligning large knowledge bases*,” pp. 572–580, 2013.

[24] A. Gruenheid, D. Kossmann, R. Sukriti, and F. Widmer, “*Crowdsourcing entity resolution: When is  $a=b$ ?*,” Eth Department of Computer Science Systems Group, 2012.

[25] L. Getoor and A. Machanavajjhala, “*Entity resolution: theory, practice & open challenges*,” Proceedings of the VLDB Endowment, vol. 5, no. 12, pp. 2018–2019, 2012.

[26] X. Chu, J. Morcos, I. F. Ilyas, M. Ouzzani, P. Papotti, N. Tang, and Y. Ye, “*Katara: A data cleaning system powered by knowledge bases and crowdsourcing*,” in Proceedings of the ACM International Conference on Management of Data (SIGMOD), SIGMOD ’15, (New York, NY, USA), pp. 1247–1261, ACM, 2015.

[27] D. Firmani, B. Saha, and D. Srivastava, “*Online entity resolution using an oracle*,” Proceedings of the VLDB Endowment, vol. 9, no. 5, pp. 384–395, 2016.

[28] S. E. Whang, P. Lofgren, and H. Garcia-Molina, “*Question selection for crowd entity resolution*,” Proceedings of the VLDB Endowment, vol. 6, no. 6, pp. 349–360, 2013.

[29] C. Gokhale, S. Das, A. Doan, J. F. Naughton, N. Rampalli, J. Shavlik, and X. Zhu, “*Corleone: Hands-off crowdsourcing for entity matching*,” Proceedings of the ACM International Conference on Management of Data (SIGMOD), pp. 601–612, 2014.

[30] S. Wang, X. Xiao, and C.-H. Lee, “*Crowd-based deduplication: An adaptive approach*,” Proceedings of the ACM International Conference on Management of Data (SIGMOD), pp. 1263–1277, 2015.

[31] V. Verroios, H. Garcia-Molina, and Y. Papakonstantinou, “*Waldo: An adaptive human interface for crowd entity resolution*,” pp. 1133–1148, 2017.

[32] A. Gruenheid and D. Kossmann, “*Cost and quality trade-offs in crowdsourcing*,” 2018.

- [33] *J. Fan, G. Li, B. C. Ooi, K. L. Tan, and J. Feng, “icrowd: An adaptive crowdsourcing framework,” in Proceedings of the ACM International Conference on Management of Data (SIGMOD), pp. 1015–1030, 2015.*
- [34] *“Nadeef/er: generic and interactive entity resolution,”*
- [35] *C. E. Rasmussen and C. K. Williams, Gaussian processes for machine learning. MIT press Cambridge, 2006.*
- [36] *H. M. Markowitz, “Foundations of portfolio theory,” Journal of Finance, vol. 46, no. 2, pp. 469–477, 1991.*
- [37] *R. T. Rockafellar and S. Uryasev, “Conditional value-at-risk for general loss distributions,” Journal of Banking & Finance, vol. 26, no. 7, pp. 1443–1471, 2002.*
- [38] *C. Acerbi and D. Tasche, “Expected shortfall: A natural coherent alternative to value at risk,” Economic Notes, vol. 31, no. 2, pp. 379–388, 2002.*
- [39] *M. Hababou, A. Cheng, and R. Falk, “Variable selection in the credit card industry,” NESUG Proc. Stat. Pharmacokinet., pp. 1–5, 2006.*
- [40] *Y. Zhang, G. Chu, P. Li, X. Hu, and X. Wu, “Three-layer concept drifting detection in text data streams,” Neurocomputing, 2017.*